Journal of Techniques, ISSN: 2708-8383, Vol. 8, No. 1, 2026, Pages 89-97
https://doi.org/10.51173/jt.v8i1.2906

JOURNAL OF TECHNIQUES

Journal homepage: http://journal.mtu.edu.iq

RESEARCH ARTICLE - MECHANICAL ENGINEERING

Interactive Modelling Strategy for Predicting the Torsional Dynamic Response of a Damper Pulley

Walid Baccar[1*], Ezzeddine Ftoutou[1], SeddiK Shiri[2], Moez Trigui[1]

[1]Mechanical Engineering Laboratory (LR99ES32), National Engineering School of Monastir (ENIM), University of Monastir, Avenue Ibn El Jazzar, B.P. 5019, Monastir, Tunisia

[2]Laboratory of Mechanics and Energy, National Engineering School of Bizerte (ENIB), University of Carthage, Menzel Abderrahmane, B.P. 7035, Bizerte, Tunisia

[*] Corresponding author E-mail: walid_baccar@yahoo.fr

Article Info.

Article history:

Received
28 February 2026

Revised
21 March 2026

Accepted
29 March 2026

Published
31 March 2026

Abstract

Damper pulleys are critical mechanical subsystems in internal combustion engines that attenuate torsional vibrations arising from cyclic combustion pressures and crankshaft torque fluctuations. Existing modelling approaches range from simple empirical or linear models to advanced numerical formulations; however, few studies systematically incorporate the combined frequency and temperature dependence of elastomer viscoelasticity with a robust experimental identification framework. The strong thermo-mechanical coupling and material nonlinearity therefore still challenge accurate prediction of torsional behavior under realistic conditions. This study proposes an interactive and novel methodology that couples analytical modelling with experimental identification to characterize the torsional dynamic response of a damper pulley in a thermos-viscoelastic context. Key contributions are: (i) identification of the elastomer complex shear modulus by dynamic mechanical analysis across an extended temperature range; (ii) implementation of these temperature-dependent constitutive parameters in a lumped-parameter torsional vibration model incorporating inertia, stiffness, and viscoelastic damping; and (iii) an iterative calibration procedure correlating analytical predictions with modal parameters extracted from instruments impact tests performed at multiple temperatures. The closed-loop identification updates model parameters systematically until the numerical predictions and experimental measurements converge. Parametric studied quantify the influence of temperature and elastomer thickness: increasing temperature or elastomer thickness reduces the first torsional natural frequency, primarily due to a drop in storage modulus and effective torsional stiffness, whereas decreasing thickness raises the resonance frequency. Predicted and measured natural frequencies differ by less than 5% across the investigated thermal domain, demonstrating the robustness formulation. The developed framework provides a validated and original basis for thermo-viscoelastic modelling, sensitivity analysis, and structural optimization of torsional vibration dampers under varying operating conditions.

Publisher: Middle Technical University

Keywords: Viscoelastic Damper; Temperature Effect; Experimental-Analytical Coupling; Torsional Vibration; Passive Damping.

1. Introduction

Damper Pulleys (DPs) were introduced in the early 20th century to reduce engine vibrations and prevent premature wear. Early designs used tuned mass dampers, while later developments incorporated materials like rubber and advanced systems such as inertia-mass and hydraulic dampers. Today, DPS are widely applied in both conventional and high-performance engines to ensure vibration control and durability. With the emergence of modern high-output engines, DPs have continued to evolve, supported by advanced modelling and simulation techniques that enable each damper to be specifically engineered according to the dynamic behavior of a given engine. Today, DPs are key components of the powertrain, designed to suppress unwanted crankshaft oscillations and to protect surrounding mechanical elements. Recent developments include the use of composite materials and electronically controlled devices capable of adapting damping levels to varying operating conditions. A damper pulley typically consists of at least two metallic parts connected by an elastomer layer that provides vibration damping. Such pulleys, designed in various configurations [1-3], have proven effective in reducing vibration levels. The scientific literature presents a wide range of approaches and theoretical models for DPs, which can generally be classified into two main categories: (i) approaches focused on characterizing the damper pulley itself, using one or two degrees-of-freedom models Honda et al. [4], independently of the transmission system in which it is installed; and (ii) approaches aimed at analyzing the dynamic behavior of transmission systems, either with or without the inclusion of DPs [5-7].

Deuszkiewicz et al. [8] and Píštěk et al. [9] developed analytical models of DPs using equations of motion combined with experimental characterisations of the damping provided by the elastomer layer. Consequently, parametric studies investigating the effects of temperature and

Nomenclature & Symbols			
C	Viscous Damping of the Pulley	K	Stiffness of the Pulley
CAD	Computer Aided Design	TVD	Torsional Vibration Damper
DMA	Dynamic Mechanical Analysis	J_1	Inertia of the Pulley
FRF	Frequency Response Function	θ	Rotation Angle Around the Axis of Rotation
E	Young Modulus	θ_e	Amplitude of the Excitation
E'	Real Part of Complex Modulus	ν	Poisson Ratio of the Rubber
E''	Imaginary Part of Complex Modulus	ω	Excitation Frequency
E*	Complex Modulus		

rotational speed on the natural frequencies and mode shapes has been carried out [10-12]. These modelling approaches enable the prediction of frequencies and mode shapes for DPs with arbitrary geometries. Other studies have examined DPs behavior, including the effects of material selection, geometrical dimensions, and stiffness properties of the elastomer used [13].

The second category addresses the dynamic behavior of mechanical systems equipped with DPs [14-17]. These studies aim to understand the vibration attenuation mechanisms induced by DPs and to optimize their performance. Kinoshita et al. [18], Takeo et al. [19], and Schwibinger et al. [20] conducted experimental investigations, either through laboratory testing or field measurements, to evaluate the effectiveness of DPs in practical applications. Their results demonstrated that elastomer-based dampers significantly reduce vibration levels, improve engine performance, and enhance passenger comfort [21].

Despite the extensive research conducted on DPs, the wide range of design parameters and the specific behavior of viscoelastic materials remain areas that require further investigation. This study is particularly important for DPs manufacturers, as it provides a validated framework to optimize design, improve vibration attenuation, and enhance engine performance and durability. The objective is to provide an engineering support tool for estimating the first natural frequency likely to be excited and to assess the influence of rubber thickness on its temperature-dependent variation. In addition, the proposed approach aims to enhance predictive capability through combined analytical modelling and experimental validation over a representative thermal operating range.

2. Interactive Methodology Strategy

Fig. 1 illustrates the proposed methodological framework based on the coupling between an analytical approach and experimental characterisation. Viscoelastic properties obtained by Dynamic Mechanical Analysis (DMA) are integrated into the analytical model, which is iteratively calibrated and validated using experimental data. This bidirectional interaction allows the development of a hybrid model that consistently combines experimental observations and analytical predictions. The methodology is systematically repeated over a range of temperatures in order to capture the temperature-dependent behaviour of the viscoelastic material and to establish a model that remains valid across the investigated thermal domain.

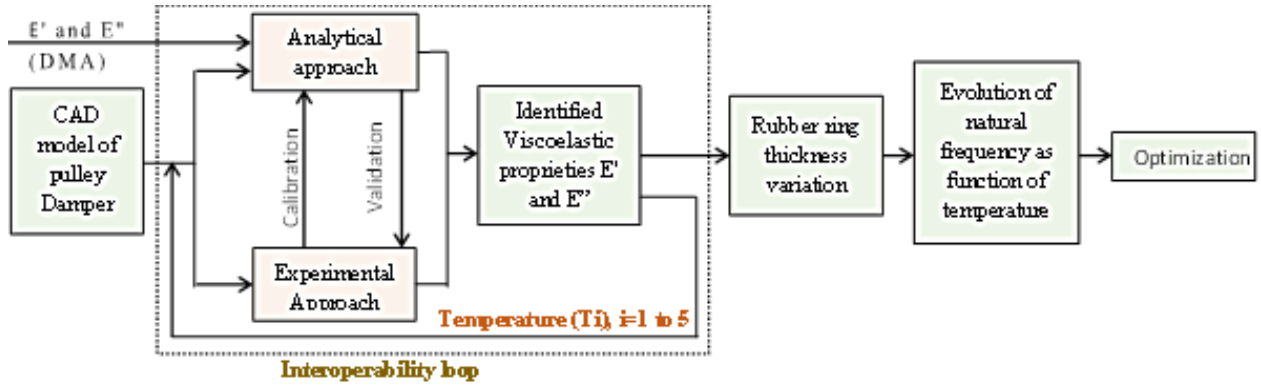

Fig. 1. Developed an interactive approach

As shown in the Fig. 1, the workflow begins by introducing the geometrical parameters of the pulley damper model, created in SolidWorks (including volume, moments of inertia, and mass), and along with the viscoelastic properties of the rubber obtained by DMA, into the analytical approach. The values from the analytical and experimental approaches are then compared, followed by calibration to minimize discrepancies. This process is iterated across different temperatures. The validated model demonstrates the influence of ring thickness on the first torsional natural frequency and enables the study of the effects of temperature variation on this frequency.

2.1. Geometric model

The damper pulley model, created using SolidWorks, is presented in Fig. 2, while its characteristics are summarized in Table 1. This pulley corresponds to a passenger vehicle application. According to the manufacture of this damper pulley, its part number is 0515G3-metalcaucho 2926, and it is installed in various internal combustion engines across multiple vehicle models. The choice of this pulley is justified by our objective to study a specific case of pulley operating under conditions where the parameters under investigation directly influence its dynamic behaviour.

Table 1. Damper pulley characteristics

Properties	Crown	Ring	Hub
E (GPa)	105	6.1	
ρ (kg/m^3)	7800	960	105
υ	0.24	0.49	7800
M (kg)	1.615	0.038	0.24
I (kg*mm^2)	8434.27	142.04	1.223
L (mm)	-	31.5	2558.9
e (mm)	-	3	-
R (mm)	-	62	-

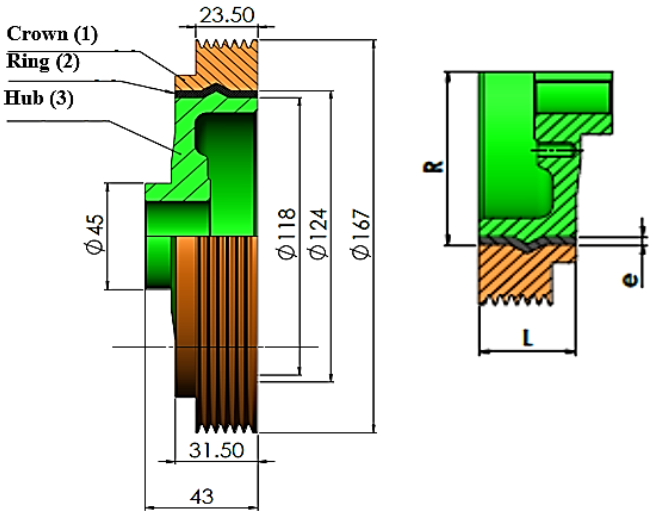

Fig. 2. CAD model of the damper pulley

2.2. Analytical model

To simplify the modelling of DPs, their dynamic behaviour can be represented using a Torsional Vibration Damper (TVD), which is a mass-spring-damper system with a single degree of freedom Silva et al. [10] and [22, 23]. This system is analogous to other oscillatory systems, except that the only degree of freedom corresponds to rotation around the crankshaft axis [24]. The damping resulting from the viscoelasticity behaviour of the intermediate ring is introduced into the model in order to evaluate the effects of temperature and rotational frequency on the system's dynamic response.

Under these assumptions, the equations of motion are expressed as in Eq. 1, accounting for the variation of the stiffness coefficient K of the intermediate ring and the viscous damping coefficient C of the TVD as functions of temperature and frequency:

$$J_1 \ddot{\theta} + C\dot{\theta} + K\theta = C\theta_e\omega\cos(\omega t) + K\theta_e\sin(\omega t) \quad (1)$$

- J_1: is the inertia of the pulley,
- θ, $\dot{\theta}$ and $\ddot{\theta}$: represent respectively the rotation angle, angular velocity, and angular acceleration about the axis of rotation, defining the considered degree of freedom,
- K: is the stiffness of the pulley,
- C: is the viscous damping of the pulley, varying with the elastomer temperature and the rotational frequency,
- θ_e: is the amplitude of the excitation,
- ω: is the excitation frequency corresponding to engine fluctuations.

The Frequency Response Function (FRF) of the system is given by Eq. 2:

$$FRF = \frac{\theta}{\theta_{cs}} = \frac{\sqrt{1+(2\psi r)^2}}{\sqrt{(1+r^2)^2+(2\psi r)^2}} \quad (2)$$

The phase shift $\varphi(\theta)$ of the transfer function is expressed by:

$$\varphi(\theta) = tg^{-1}\left(\frac{2\psi r^3}{1-r^2+(2\psi r)^2}\right) \quad (3)$$

- $r = \frac{\omega}{\omega_0}$ denoting the reduced frequency,
- $\omega_0 = \sqrt{\frac{K}{J_1}}$ is the natural frequency, and
- $\psi = \frac{C}{2\sqrt{KJ_1}}$ is the intrinsic damping ratio of the pulley.

2.3. Incorporation of viscoelastic properties

The stiffness modulus of the elastomer ring is introduced into the dynamic model through the complex modulus *E** [25]. This modulus, which characterizes the material response under small-amplitude vibrational loading, is defined in Eq. 4:

$$E^* = E' + jE'' = f(T, f, \varepsilon) \quad (4)$$

In general, the complex modulus E* is determined experimentally through DMA. The real part of E′ represents the storage modulus, associated with the elastic energy stored during deformation, while the imaginary part E″ corresponds to the loss modulus, which quantifies the energy dissipation capacity of the elastomer. In the present study, the values of E' and E" introduced into the analytical model were obtained from DMA data reported in the literature [6]. The experimental parameters T, f, and ε refer, respectively, to the temperature, loading frequency, and dynamic strain applied during DMA testing.

The torsional stiffness of the rubber ring in a damper pulley is given by Eq. 5: (see Fig. 2)

$$K = \frac{2\pi R^3 LG}{e} \quad (5)$$

- L: denotes the ring width
- R: The radius
- e: the ring thikness

Considering the viscoelastic behaviour of the rubber ring, the stiffness K and damping coefficient C, which depend on temperature, frequency, and dynamic strain, can be expressed as Eq. 6:

$$K = \frac{2\pi R^3 L}{e(1+\nu)} E' \text{ and } C = \sqrt{K J_1}\frac{E''}{E'} \quad (6)$$

ν represents the Poisson ratio of the rubber. Taking into account the viscoelasticity of the rubber ring, the equation of motion becomes:

$$J_1 \ddot{\theta} + C\dot{\theta} + K\theta = C\theta_e \omega \cos(\omega t) + K\theta_e \sin(\omega t) \quad (7)$$

Table 2 presents the values of different properties of the material of the rubber used in the analytical approach.

Table 2. Mechanical and physical properties of the rubber material

Properties	Value at 20°C
Hardness	45 Shore
Young modulus E	8.54 (GPa)
ρ	960 (kg/m^3)
υ	0.49

2.4. Experimental approach

A schematic representation of the experimental setup is shown in Fig. 3. The tested damper pulley is similar to the one considered in the analytical model. The hub of the pulley is clamped to a rigid metallic structure only through its shaft, while an accelerometer is mounted on the pulley crown (Fig. 4). The experiment consists of exciting the pulley using an impact hammer and measuring the FRF via the accelerometer.

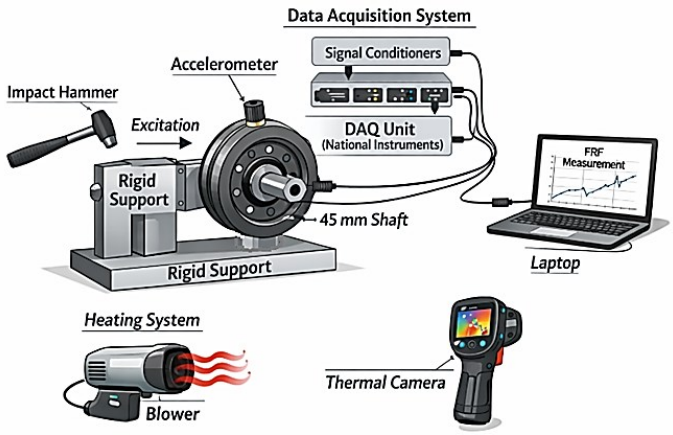

Fig. 3. Damper pulley testing setup schematic

The data acquisition system comprises an accelerometer, signal conditioners, and a National Instruments data acquisition system (DAQ), which were used to record the vibration response of the pulley damper. The sampling frequency of the acquired signals was set to 12 kHz to capture the first natural frequencies of the pulley damper. These measurements are repeated over a range of temperatures. Moreover, to ensure reliable experimental characterisation of the damper pulley, the previously described tests were repeated five times, and the average frequencies were determined.

An enclosure chamber was employed to maintain a uniform temperature throughout the pulley volume. For this purpose, a heating system equipped with a blower and thermal camera sensor was employed to control and monitor the temperature. Experimental equipment consisted of a PCB impact hammer Type 086C03, a B&K accelerometer, B&K Charge Converter, a data acquisition card NI USB-9234, a clamping system, and a computer. The characteristics of the equipment required are listed in Table 3.

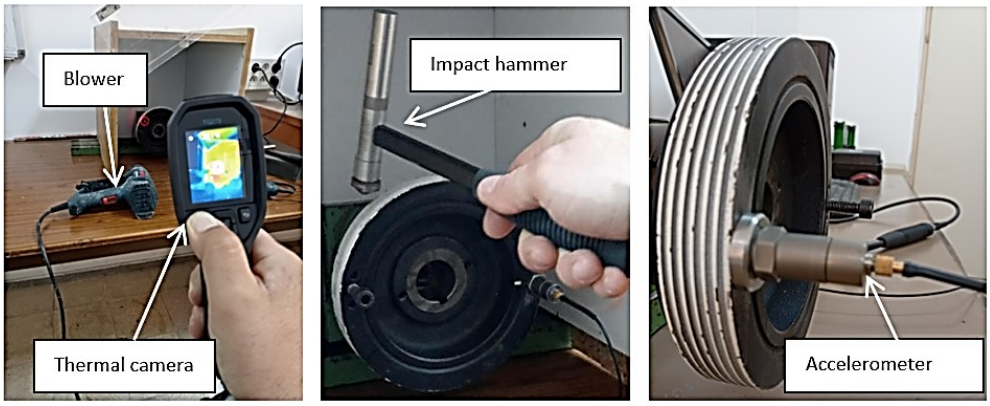

Fig. 4. Experiment of modal analysis and temperature measurement testing

Table 3. Equipment characteristics

Model	PCB Impact hammer 086C03	B&K Accelerometer Type 4382	B&K Charge Converter Type 2646
Sensitivity	2.25 mV/N	3.175 pC/ms²	Adjustable (1 mV/pC)
Resonance frequency	22 kHz	27.2 kHz	> 100 kHz
Measurement range	± 2224 N pC	50 km/s² pC	±10 V output
Sensing element	Quartz	PZ 23	-
A/D card NI USB-9234			
Parameter		Specification	
Product Type		Dynamic Signal Acquisition (DSA) Module	
Maximum Sampling Rate		51.2 kS/s per channel (simultaneous)	
Input Voltage Range		±5 V	
IEPE Excitation		Yes (Integrated Electronics Piezoelectric)	
Operating Temperature Range		−40 °C to +70 °C (typical)	

3. Results and Discussion

3.1. Experimental results

In accordance with the procedure described previously in section 2, the first natural frequency of the pulley damper was determined at different temperatures, as shown in Fig. 5. The corresponding values are summarized in Table 4. These results indicate that the first natural frequency of the damper pulley decreases as temperature increases.

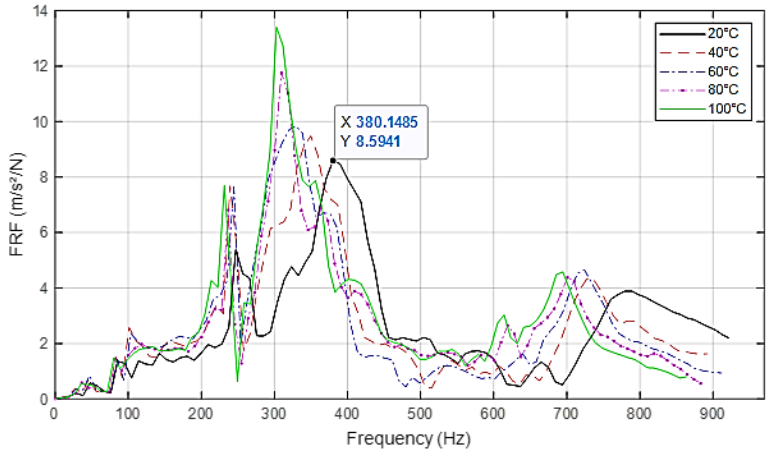

Fig. 5. Experimental first natural frequency of the pulley damper at different temperatures

Table 4. Variation of the first natural frequency versus temperature

Temperature °C	20	40	60	80	100
First natural frequency (Hz)	380.15	349.74	329.13	309.52	302.72

3.2. Results of the calibration of E' and E'' based on experimentation

Based on the methodology described previously, a calibration step of the elastic modulus E' and E'' was carried out. Table 5 presents a comparison between the values initially introduced in the analytical model and those obtained after calibration. It should be noted that the values

of E' and E'' depend on the rotational frequency of the pulley, which ranges from 1 to 300 Hz and corresponds to the actual operating frequencies of this component. Fig. 6 illustrates the evolution of the calibrated E' and E'' modulus as a function of the pulley's rotational frequency.

3.3. Analytical analysis

Once both moduli have been calibrated for the studied pulley, it becomes possible to initiate the investigation of the thickness effect. However, before this step, the accuracy of the analytical model must be assessed. Fig. 7 shows the variation of the first natural frequency predicted by the analytical model as a function of the rotational frequency. From these results, it is worth noting that a slight decrease in the maximum amplitude and phase of the Frequency Response Function is observed with increasing temperature. Furthermore, the first natural frequency is inversely related to temperature, decreasing from 360.33 Hz at 20°C to 334.67 Hz at 40°C, 314.5 Hz at 60°C, 295.83 Hz at 80°C, and finally 290.5 Hz at 100°C.

The discrepancy between these values and the experimental results is reported in Table 6. As indicated in this table, the calculated error is on the order of 5%, highlighting good agreement between the analytical model and the experimental data. These results confirm the validity of the E' and E'' equations and allow their use in the study of the influence of thickness on the first natural frequency.

Table 5. Empirical equations for E' and E" derived from F.Silva's and from the experiment

	Derived from F.Silva's study		**Obtained from the present experiments**	
Temperature °C	E' (MPa)	E" (MPa)	E' (MPa)	E" (MPa)
20	$6{,}55f_{req}^{0{,}0814}$	$5{,}79f_{req}^{0{,}0156} - 4{,}81$	$6{,}55f_{req}^{0{,}0650}$	$5{,}79f_{req}^{0{,}014} - 4{,}81$
40	$5{,}68f_{req}^{0{,}0815}$	$5{,}41f_{req}^{0{,}0163} - 4{,}58$	$5{,}68f_{req}^{0{,}0651}$	$5{,}41f_{req}^{0{,}0147} - 4{,}58$
60	$5{,}02f_{req}^{0{,}0820}$	$6{,}17f_{req}^{0{,}0141} - 5{,}47$	$5{,}02f_{req}^{0{,}0656}$	$6{,}17f_{req}^{0{,}0125} - 5{,}47$
80	$4{,}49f_{req}^{0{,}0808}$	$6{,}07f_{req}^{0{,}0139} - 5{,}49$	$4{,}49f_{req}^{0{,}0644}$	$6{,}07f_{req}^{0{,}0123} - 5{,}49$
100	$4{,}27f_{req}^{0{,}0835}$	$6{,}34f_{req}^{0{,}0137} - 5{,}81$	$4{,}27f_{req}^{0{,}0671}$	$6{,}34f_{req}^{0{,}0121} - 5{,}81$

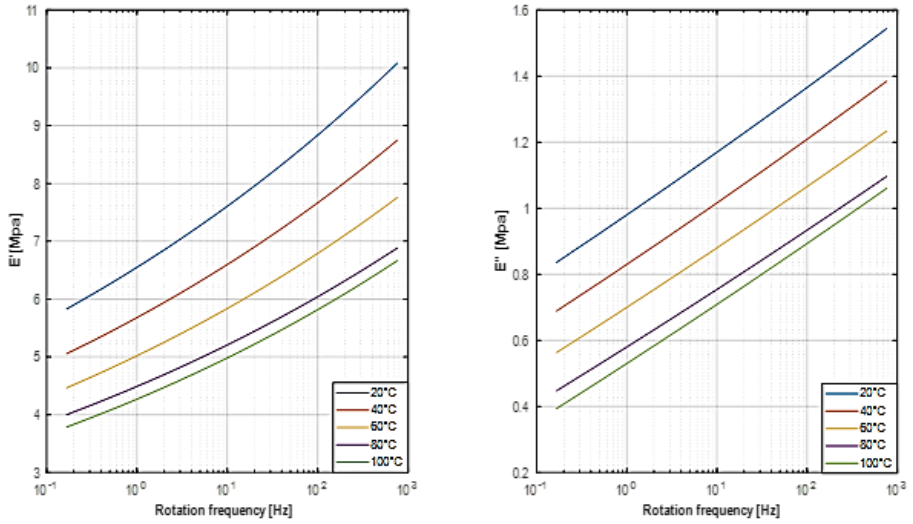

Fig. 6. Evolution of E' and E" as function of the pulley's rotational frequency

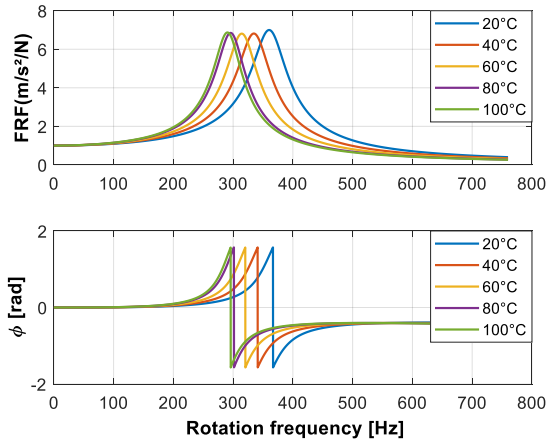

Fig 7. Evolution of the First natural frequency versus temperature

Table 6. Relative error between analytical and experimental results

Temperature °C	First natural frequency (Hz)		Relative error in %
	Experimental values	Analytical values	
20	380.15	360.33	5.21
40	349.74	334.67	4.50
60	329.13	314.5	4.65
80	309.52	295.83	4.62
100	302.72	290.5	4.20

By using the calibrated empirical equations presented in Table 5 along with the analytical model, the evolution of the stiffness and damping as a function of the excitation rotational frequency can be represented for different temperatures (Fig. 8). It can be observed that both C and K decrease significantly as the temperature increases.

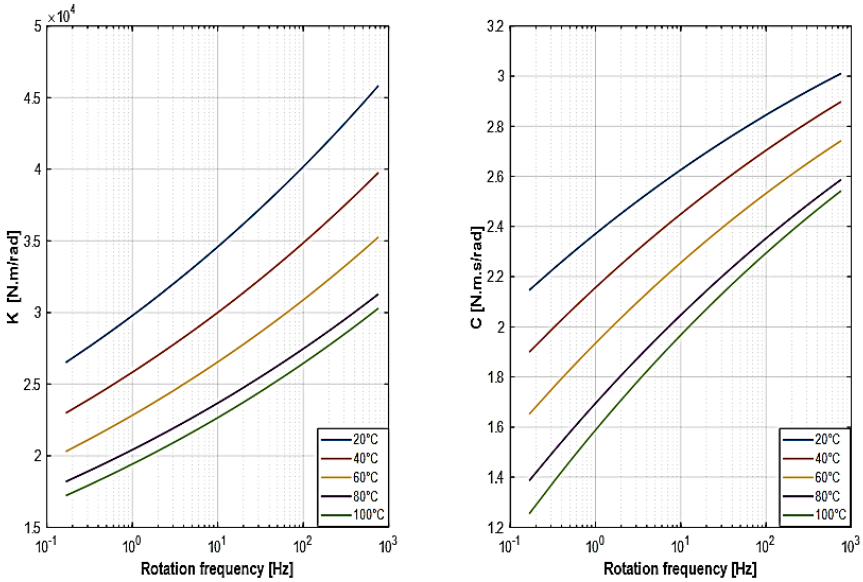

Fig. 8. Variation of stiffness K and damping C versus temperature

3.4. Influence of rubber thickness

To study the influence of the rubber ring thickness on the natural frequency, the hub radius was first kept constant while varying the ring thickness, and then the crown radius was fixed while the ring thickness was varied. Fig. 9 illustrates the result of the parametric study of thickness on the variation of natural frequency at 20 °C. The results show that the natural frequency decreases as the ring thickness increases. This indicates that the stiffer the damper, corresponding to a smaller rubber ring thickness, the higher its natural frequency.

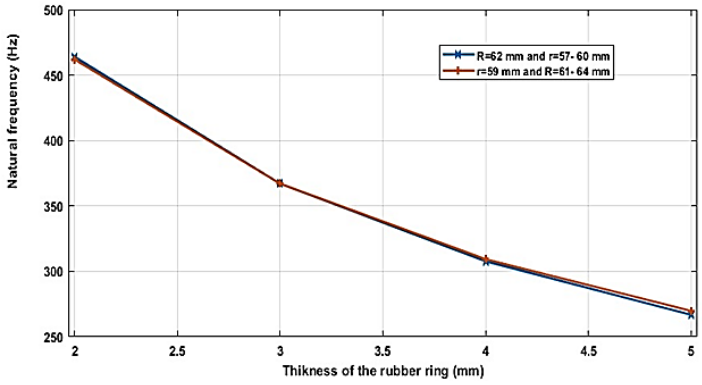

Fig. 9. Effect of rubber thickness on the first natural frequency at 20 °C

3.5. Thickness and temperature effect

The behaviour of the damper pulley at different operating temperatures and across a range of rubber ring thicknesses is shown in Fig. 10. The results clearly indicate that the natural frequency of the damper pulley increases for smaller ring thicknesses and decreases significantly for larger ones. This trend occurs because a thinner ring thickness makes the pulley stiffer, thereby raising the natural frequency, whereas a thicker ring reduces stiffness and lowers it. Furthermore, the influence of temperature on the natural frequency is inversely proportional, as the ring material behaves more rigidly at low temperatures and becomes more elastic at higher temperatures.

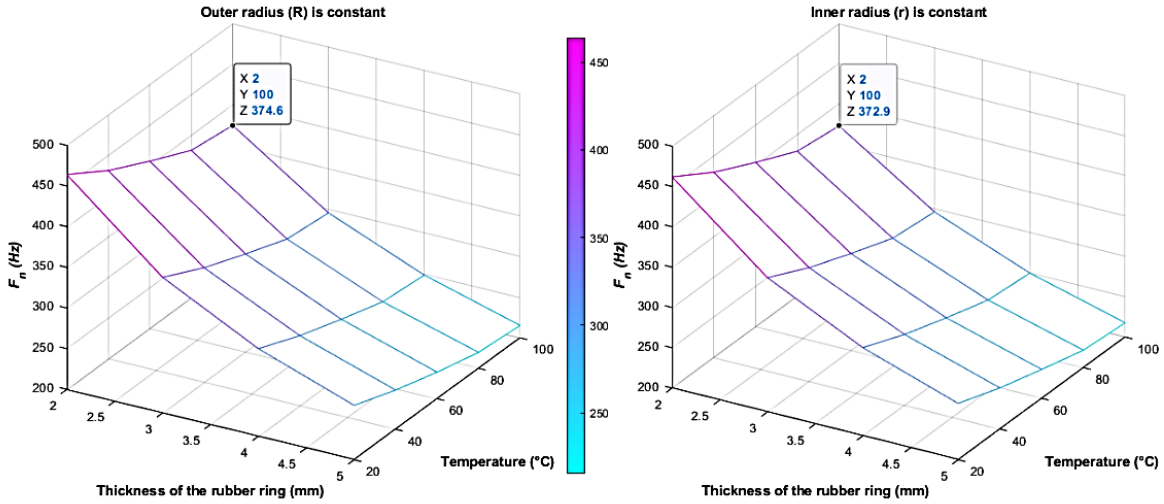

Fig. 10. Effect of rubber thickness and temperature on the first natural frequency at 20 °C

4. Conclusions

In this research, an interactive and iterative methodology combining analytical modelling and experimental identification was proposed to describe the torsional dynamic behaviour of a damper pulley. The model, based on a lumped-parameter approach, was calibrated using experimental modal data to ensure consistency with the physical behaviour of the system. The parametric analysis, revealed a clear inverse relationship between rubber ring thickness and the first torsional natural frequency. Increasing the ring thickness reduced the equivalent torsional stiffness, leading to a lower resonance frequency, whereas decreasing thickness increased stiffness and shifted the resonance to higher frequencies. Temperature effects were also significant: low temperatures increased the elastomer rigidity and natural frequencies, while higher temperatures reduced stiffness and frequency. The maximum deviation between analytical and experimental results remains around 5%, signifying the robustness of the identification procedure and the validity of the calibrated E' and E'' expressions. Overall, the proposed methodology provided an effective engineering framework for analysing and optimizing the dynamic performance of damper pulleys under thermo-mechanical conditions.

Acknowledgment

The authors wish to express their sincere appreciation to the Mechanical Engineering Laboratory (LR99ES32) at the National Engineering School of Monastir (ENIM), University of Monastir, for providing laboratory facilities and technical assistance throughout this study.

References

[1] V. Ganesan, Internal Combustion Engines. New Delhi, India: Tata McGraw-Hill Education, 2003.
[2] Filipović et al., "Preliminary selection of basic parameters of different torsional vibration dampers intended for use in medium-speed diesel engines," Trans. FAMENA, vol. 36, pp. 79-92, 2012.
[3] Tomohito, "Damper pulley manufacturing method and damper pulley manufacturing apparatus," U.S. Patent 20160/102749 A1, 2016.
[4] Y. Honda and T. Saito, "Dynamic characteristics of torsional rubber dampers and their optimum tuning," SAE Tech. Paper 870580, 1987, https://doi.org/10.4271/870580 .
[5] K. Wakabayashi et al., "Torsional vibration damping of diesel engine with rubber damper pulley," JSME Int. J., Ser. C, vol. 38, no. 4, pp. 670-678, Nov. 1995, https://doi.org/10.1299/jsmec1993.38.670.
[6] Z. Zhang et al., "Variable damping mechanism and verification of the torsional damper for a parallel-series hybrid electric vehicle," J. Vibroeng., 2024, https://doi.org/10.21595/jve.2024.24201.
[7] T. Kodama and Y. Honda, "A study on the modeling and simulation method of torsional vibration considering dynamic properties of rubber parts for engine crankshaft system with rubber damper pulley," Int. J. Mech. Eng. Robot. Res., vol. 9, no. 7, Jul. 2020, https://doi.org/10.18178/ijmerr.9.7.1007-1011.
[8] P. Deuszkiewicz and J. Pankiewicz, "Nonlinear model of rubber torsional vibration damper," Vibroeng. PROCEDIA, vol. 6, pp. 78-82, 2015.
[9] V. Píštěk et al., "An unconventional rubber torsional vibration damper with two degrees of freedom," Vibroeng. PROCEDIA, vol. 13, pp. 136-141, 2017, https://doi.org/10.21595/vp.2017.19042.
[10] C. A. F. Silva et al., "Dynamics of torsional vibration damper (TVD) pulley, implementation of rubber elastomeric behaviour, simulations, and experiments," Mech. Ind., vol. 20, no. 2, p. 142, 2019, https://doi.org/10.1016/j.mechmachtheory.2019.103583.
[11] L. Manin, R. Dufour, and S. Schultz, "Pulley torsional vibration damper characterization," Mech. Ind., vol. 14, no. 3, pp. 151-155, 2013, https://doi.org/10.1051/meca/2013057.
[12] Y. A. Yucesan et al., "Adjusting a torsional vibration damper model with physics-informed neural networks," Mech. Syst. Signal Process., vol. 154, Mar. 2021, Art. no. 107602, https://doi.org/10.1016/j.ymssp.2020.107552.
[13] C. R. Stahl, "Development and effects of viscous type dampers on applications other than engine crankshafts," SAE Trans., vol. 97, no.

5, pp. 316-318, 1988, https://doi.org/10.4271/880823.
[14] S. Mendes et al., "Analysis of torsional vibration in internal combustion engines: Modelling and experimental validation," Proc. Inst. Mech. Eng., K, J. Multi-body Dyn., vol. 222, no. 2, pp. 155-165, 2008, doi: 10.1243/14644193JAMD189.
[15] M. H. Sar, O. S. Barrak, A. S. Al-Adili, S. K. Hussein, and A. K. Hussein, “Study the effect of filler material on microstructure of welding the carbon steel in shielded metal arc welding,” Journal of Mechanical Engineering Research and Developments, vol. 43, no. 3, pp. 408–416, 2020.
[16] W. Homik and P. Grzybowski, "The simulation model of small-dimension rubbery torsional vibration damper," Vibroeng. PROCEDIA, vol. 6, pp. 78-82, 2015.
[17] K. Yadav et al., "Critique of torsional vibration damper (TVD) design for powertrain NVH," SAE Tech. Paper 2017-26-0217, 2017, https://doi.org/10.4271/2017-26-0217.
[18] M. Kinoshita, "An experimental study of a torsional/bending damper pulley for an engine crankshaft," SAE Trans., vol. 98, pp. 1605-1615, 1989, https://doi.org/10.4271/891127.
[19] T. Naganuma, H. Okamura, and K. Sogabe, "Experiments and analyses of the three-dimensional vibrations of the crankshaft and torsional damper in a four-cylinder in-line high speed engine," SAE Trans. J. Passenger Cars, vol. 106, no. 6, pp. 3011-3022, 1997, https://doi.org/10.4271/971996..
[20] P. Schwibinger, D. Hendrick, W. Wu, and Y. Imanishi, "Reduction of vibration and noise in the powertrain of passenger cars with elastomer damper," SAE Trans. J. Passenger Cars, vol. 100, no. 6, pp. 787-795, 1991, https://doi.org/10.4271/910616.
[21] L. Drápal and P. Novotný, "Torsional vibration analysis of crank train with low friction losses," J. Vibroeng., vol. 19, no. 8, pp. 6078-6090, Dec. 2017, https://doi.org/10.21595/JVE.2017.17876.
[22] H. Dresig and F. Holzweißig, Dynamics of Machinery - Theory and Applications. Berlin, Germany: Springer, 2010.
[23] M. I. Friswell, J. E. T. Penny, S. D. Garvey, and A. W. Lees, Dynamics of Rotating Machines. Cambridge, U.K.: Cambridge Univ. Press, 2010.
[24] H. Blanc, "Dynamique des rotors en torsion: Étude des amortisseurs de torsion," Tech. l'Ingénieur, Ref. BM5124 V1, 2000.
[25] J. D. Ferry, Viscoelastic Properties of Polymers, 3rd ed. New York, NY, USA: John Wiley & Sons, 1980.